

A new compact young moving group around V1062 Sco

Siegfried Röser^{1,2}, Elena Schilbach^{1,2}, Bertrand Goldman^{3,4}, Thomas Henning³, Attila Moor⁵, and Aliz Derekas^{5,6}

¹ Zentrum für Astronomie der Universität Heidelberg, Landessternwarte, Königstuhl 12, 69117 Heidelberg, Germany

² Zentrum für Astronomie der Universität Heidelberg, Mönchhofstraße 12-14, 69120 Heidelberg, Germany
e-mail: roeser@ari.uni-heidelberg.de, elena@ari.uni-heidelberg.de

³ Max-Planck-Institut für Astronomie, Königstuhl 17, 69117 Heidelberg, Germany e-mail: goldman@mpia.de

⁴ Observatoire astronomique de Strasbourg, Université de Strasbourg - CNRS UMR 7550, 11 rue de l'Université, 67000, Strasbourg, France

⁵ Konkoly Observatory, Research Centre for Astronomy and Earth Sciences, Hungarian Academy of Sciences, H-1121 Budapest, Konkoly Thege Miklós út 15-17, Hungary

⁶ ELTE Eötvös Loránd University, Gothard Astrophysical Observatory, Szombathely, Hungary

Received 30 October 2017; accepted 27 December 2017

ABSTRACT

Aims. We are searching for new open clusters or moving groups in the Solar neighbourhood.

Methods. We used the Gaia-TGAS catalogue, cut it into narrow proper motion and parallax slices and searched for significant spatial over-densities of stars in each slice. We then examined stars forming over-densities in optical and near-infrared colour-magnitude diagrams to determine if they are compatible with isochrones of a cluster.

Results. We detected a hitherto unknown moving group or cluster in the Upper Centaurus Lupus (UCL) section of the Sco-Cen OB-association at a distance of 175 pc from the Sun. It is a group of 63 co-moving stars with ages of less than 10 to about 25 Myr. For the brightest stars, which are present in the Gaia-TGAS catalogue the mean difference between kinematic and trigonometric distance moduli is -0.01 mag with a standard deviation of 0.11 mag. Fainter cluster candidates are found in the HSOY catalog, where no trigonometric parallaxes are available. For a subset of our candidate stars, we obtained radial velocity measurements at the MPG/ESO 2.2-metre telescope in La Silla. Altogether we found twelve members with confirmed radial velocities and parallaxes, 31 with parallaxes or radial velocities, and 20 candidates from the convergent point method. The isochrone masses of our 63 members range from $2.6 M_{\odot}$ to $0.7 M_{\odot}$.

Key words. Open clusters and associations: general – individual: Upper Centaurus Lupus – Stars: formation – Stars: protostars – Proper motions – Parallaxes

1. Introduction

For more than a century, the Scorpius-Centaurus OB-association (Sco-Cen) has been studied as a moving group of early-type stars. Blaauw (1964) divided the huge nearby association into three subgroups, Upper Scorpius, Upper Centaurus Lupus (UCL), also known as Sco OB2_3, and Lower Centaurus Crux. After ESA's Hipparcos mission, accurate proper motions and trigonometric parallaxes became available for many early-type stars in Sco-Cen. This material has been used by de Zeeuw et al. (1999) for their fundamental paper on OB-associations.

Among the Hipparcos objects in the UCL subgroup of Sco-Cen, de Zeeuw et al. (1999) identified 221 members in this field, with a mean distance of 140 ± 2 pc, 66 B, 68 A, 55 F, 25 G, six K, and one M-type star. They also noted that the star-forming regions associated with the Lupus clouds contained several tens of low-mass pre-main-sequence stars with estimated ages of ≈ 3 Myr (see the references in de Zeeuw et al. 1999). These star-forming regions (SFR) cover most of UCL, except a small area in the south-eastern corner of UCL. It is in this area where we found a compact, young moving group of stars while searching for open clusters in the TGAS catalogue (Michalik et al. 2015; Lindegren et al. 2016).

The first Gaia data release (Gaia-DR1, Gaia Collaboration et al. 2016), and especially the publication of TGAS with its high-precision proper motions and trigonometric parallaxes fos-

tered work on open clusters and moving groups by a number of authors. Without aiming for completeness we mention here the work performed by Gaia Collaboration et al. (2017) on nearby open clusters and of Randich et al. (2017) who, combining information from Gaia-DR1 and the Gaia-ESO Survey (Gilmore et al. 2012) data, derive new distances and ages of eight nearby open clusters. Oh et al. (2017) used the TGAS catalogue to search for high-confidence comoving pairs of stars. In doing so they find some ten thousand comoving star pairs with separations as large as 10 pc. They also find larger groups corresponding to known open clusters and OB associations and several new comoving groups.

Studying the structure and the behaviour of moving groups may shed light on the process of star formation in associations. We are guided by the statement by Richard Larson (Larson 2002) in his summary during the conference "Modes of Star Formation and the Origin of Field Populations": "When associations disperse, they retain some kinematic coherence because their internal motions are relatively small, and they then become moving groups or streams. The weak-lined T Tauri stars found by X-ray observations that were discussed at this meeting probably represent some of the remnants of associations that are just now dissolving into the field and becoming moving groups." So, it was worthwhile to study our new moving group in more detail as all ingredients discussed by Larson are in place, an associa-

tion, a good number of T Tauri and weak-line T Tauri stars, and a moving group.

In this paper we describe in Section 2 how we detected this group, as well as the spectroscopic follow-up measurements we carried out with the FEROS instrument at the MPG/ESO 2.2 m Telescope in La Silla to obtain radial velocities and stellar parameters. In Section 3 we provide a discussion of the properties of the newly found group. Then, in Section 4 we compare our new group with the star-forming areas in the other parts of UCL, and a short summary concludes the paper.

2. Detection of the V1062 Sco moving group

2.1. Astrometric detection

After the first Gaia data release in September 2016, we performed a cluster search programme similar to the one described in Röser et al. (2016), but with TGAS replacing the Tycurat catalogue which we used originally. In brief the method consists in cutting the TGAS catalogue into slices as follows: in proper motion space we place a grid with grid points (i, k) at each integer value (in mas/y) from -50 mas/y to $+50$ mas/y in both proper motion components. A slice at (i, k) contains all stars for which $(\mu_\alpha \cos \delta - i)^2 + (\mu_\delta - k)^2 \leq 1.5^2 (\text{mas/y})^2$ holds. For each slice, we then check the distribution of its stars over the sky and search for possible overdensities which can be considered as candidates of clusters or moving groups.

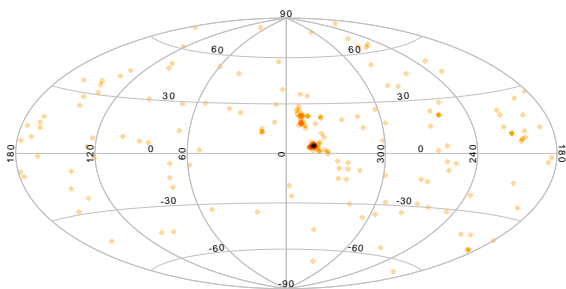


Fig. 1. Sky map (in Galactic coordinates) showing the stars from the TGAS catalog with parallaxes between 5 and 10 mas and in the proper motion slice around $(\mu_\alpha \cos \delta, \mu_\delta) = (-12, -22)$ mas/y. For further information on the selection see text.

The availability of the TGAS parallaxes allows us to improve the effectivity of the method by cutting the catalogue into parallax slices, too. Since we are especially interested in finding unknown clusters in the vicinity of the Sun, we consider a parallax slice between 5 mas and 10 mas which contains the stars between 100 and 200 pc from the Sun. Compared to the full TGAS sky with some 2 million stars this parallax slice only includes 160,000 stars. The latter is then cut into proper motion slices. In Fig. 1 we display a sky map in Galactic coordinates of the proper motion slice $(i, k) = (-12, -22)$ mas/y which only contains 159 stars. Here we found a hitherto unknown overdensity containing 25 stars (of 159) in a radius of 2.5 degrees around $(l, b) = (343.6, +4.3)$ in UCL. The fainter filamentary structure north of the overdensity may also be a substructure in Sco-Cen, but has not yet been investigated by us. Our newly found overdensity in the south-eastern corner of UCL occupies an area which is void on the ^{12}CO map from Tachihara et al. (2001). We show its location in detail on Fig. 2. Also, the trigonometric parallaxes of these 25 stars show a narrow range between 5.3 and

6.3 mas in TGAS (cf. Fig7), we henceforth refer to this overdensity of co-moving stars as the V1062 Sco Moving Group (V1062 Sco MG) according to its prominent member V1062 Sco, postponing the discussion if V1062 Sco is a true member or not to Section 3.4. Parallel to our finding of this new moving group this object has been detected in the above-mentioned paper by Oh et al. (2017) as their "Group 11", but without further discussion.

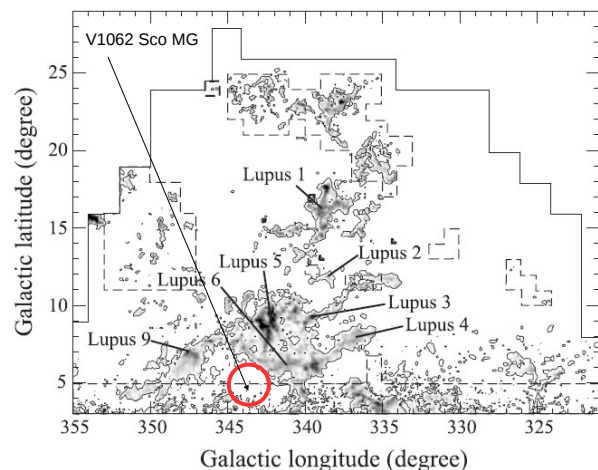


Fig. 2. The location of the V1062 Sco Moving Group (red circle) overlaid to the ^{12}CO map from Tachihara et al. (2001). The radius of the circle is 2.75° or 8.4 pc at a distance of 175 pc and roughly corresponds to the extent of the group.

2.2. Radial velocities and stellar parameters

In order to get additional confirmation for the existence of the V1062 Sco MG, we carried out FEROS observations at the MPG/ESO 2.2 m Telescope in July 2017 and determined radial velocities (RV) for a subset of possible moving group candidates. FEROS is a fiber-fed, high-resolution (48,000) cross-dispersed optical spectrograph mounted on the MPG/ESO 2.2-metre telescope in La Silla (Kaufer et al. 1999). FEROS has two set-ups: one of its two fibers points to the science target, and the second points either to a calibration lamp for better wavelength calibration, or to the sky. For brighter targets, we used both set-ups, for fainter targets only the sky set-up. We found that for our observations, the wavelength calibration errors are a minor contributor to the error budget. The observing log is given in Table A.4.

To reduce the spectra we used the CERES pipeline (Brahm et al. 2017), a reduction and extraction pipeline dedicated to échelle spectrographs. In a nutshell, for each of our three observing nights, CERES identifies the calibration files and obtains a master bias and dark frames through median filtering. The flat field is not removed at this stage but instead the blaze function obtained from continuum lamp frames is divided after extraction, which also corrects the column-averaged pixel-to-pixel variations of the CCD. It then identifies the order traces and fits them with a high-order polynomial. It measures the scattered light in the inter-order zones, interpolating over the spectra and performs a 2-D median filtering of the resulting map. After subtraction of the scattered light, the spectra are optimally extracted. The spectra are wavelength-calibrated using the ThAr lamp spectra, observed either simultaneously with the target, or during the afternoon.

CERES measures radial velocities by cross-correlating the spectra with binary masks indicating the narrow absorption lines, following Mayor et al. (2003). As CERES is optimized for late-type stars in its standard configuration, it provides masks corresponding to G2, K5 and M2 spectral types. Measurements of early-type stars is notoriously difficult as their spectra exhibit few absorption lines which are considerably broadened by stellar rotation. In the following we deal only with spectra of candidates with effective temperatures smaller than 7000 K. The uncertainties on the RV is determined as a function of the signal-to-noise ratio (SNR) at the Mg-triplet wavelength and the width of the cross-correlation function (CCF), with parameters determined from a Monte-Carlo simulation using degraded high SNR spectra. The measurements are reported in Table A.4. For targets with multiple observations we report the weighted average and the error on the mean of all the available measurements and list these stars in Table A.5. The dispersion of these individual observations roughly confirms the uncertainties derived from the SNRs.

To obtain the stellar parameters, we applied the ZASPE (Brahm et al. 2016) pipeline. The pipeline is optimized to use the spectral library of Brahm et al. (2016), created in order to reduce the biases in the stellar parameters with respect to the measurements of SWEET-Cat (Santos et al. 2013). This library covers a range of stellar temperatures up to 7000 K. The precision of the parameters can be estimated from the repeated observations of some targets, typically a few 0.1 dex in $\log g$, 0.1 dex in $[\text{Fe}/\text{H}]$, 200 m/s in $v \sin i$, a few dozens Kelvin in T_{eff} . Average values of these parameters are given in Table A.5. Our cluster members or candidates (m(4d) to m(6d), see Section 3.1) have a mean metallicity of 0.04 dex, with a spread of 0.1 dex. Their rotational velocity ranges from 5 to 80 km/s. Only one cluster candidate member shows H_{α} emission, namely star 25, which also displays (stronger) absorption. This general lack of emission, indicating no accretion, is consistent with the age range determined from the isochrones (see Section 3.2).

2.3. Phase space coordinates

For eleven out of the 25 kinematic candidate stars mentioned in Sec. 2.1 we obtained well-determined radial velocities with formal errors less than 1 km/s. Their RV pile up between 1.0 km/s to +3.6 km/s and give $RV_{\text{mean}} = +2.24 \pm 0.85$ km/s. Moreover, their parallaxes turned out to be within a narrow range between 5.4 mas and 6.2 mas, corresponding to a mean distance from the Sun of 175 ± 7 pc. For these stars we now have the complete set of 6-D phase space coordinates based on direct observations. Hence we compute the mean space coordinates and velocities of the group in barycentric Galactic coordinates to be:

$$(X, Y, Z, U, V, W) = (167.20, -49.14, 13.44, -3.80, -19.96, -4.06). \quad (1)$$

Here the X-axis points to the Galactic centre, the Y-axis to the direction of Galactic rotation and the Z-axis points to the Galactic North Pole. U, V, W are the corresponding components of the space velocity. The standard deviation in the 3 components of the space velocity is rather small $(\sigma_U, \sigma_V, \sigma_W) = (0.7, 0.9, 0.3)$ km/s. The individual residuals in velocity space do not show systematic effects such as rotation or expansion. The standard deviation sets an upper limit of 1 km/s for the one-dimensional velocity dispersion of the group, and we will show in the discussion in Sec. 3.1 that this is large compared to the formal error at least for that component of the tangential velocity which is perpendicular to the direction to the convergent point.

3. Properties the V1062 Sco Moving Group

We can use the phase space coordinates (1) of the V1062 Sco moving group to perform a search of its members. This can be done on the basis of the convergent point (CP) method we have applied to find members in the Hyades cluster (Röser et al. 2011; Goldman et al. 2013). In case of the V1062 Sco moving group, we extended the search to a distance of 10 pc around the centre $(X, Y, Z) = (167.20, -49.14, 13.44)$ from (1). Using the proper motions given in TGAS, the method predicts kinematic parallaxes ϖ_{kin} , as well as the velocity components in the tangential plane parallel and perpendicular to the direction of the convergent point. In the ideal case of an exactly parallel space motion the perpendicular component has to be zero. Taking into account a possible internal velocity dispersion and the accuracy of the input data, we allowed a maximum of 3 km/s for the perpendicular velocity component. With these restrictions we found 35 TGAS stars as kinematic candidates of the moving group. Further we required that the difference between the predicted kinematic parallaxes ϖ_{kin} and the observed trigonometric parallaxes ϖ_{trig} from TGAS to be smaller than the mean error of this difference, i.e.

$$|\varpi_{\text{kin}} - \varpi_{\text{trig}}| < (\sigma_{\varpi_{\text{kin}}}^2 + \sigma_{\varpi_{\text{trig}}}^2 + 0.3^2)^{1/2}, \quad (2)$$

where 0.3 mas was taken as a possible systematic error of trigonometric parallaxes (Lindegren et al. 2016). The application of the restriction (2) deletes two candidates, so we finally retained 33 kinematic members in our group confirmed by their trigonometric parallaxes. We publish them in Table A.1 available as on-line material together with the paper.

In order to find fainter candidates of the V1062 Sco moving group, we also used the HSOY catalogue (Altmann et al. 2017). HSOY was constructed by using Gaia-DR1 positions as an additional epoch together with PPMXL positions and proper motions to obtain formally improved proper motions. Although HSOY may have significant systematic proper motion errors over the sky, these should be unimportant for work in small areas of some tens of square degrees. We restricted our search within HSOY to $G \leq 14$ mag that yielded 17 million stars; this subset is called HSOY14 in the following. This restriction was driven by the fact that the moving group is located south of declination -30 degrees and the quality of the proper motions in HSOY for fainter stars deteriorates in this quarter of the sky. Using the convergent point method with the phase space coordinates (1) we derived kinematic parallaxes, which, however, cannot yet be verified by the trigonometric parallax observations. So, as in the case of the TGAS stars, the distance moduli and absolute magnitudes are derived from kinematic parallaxes. The CP method yielded 149 candidates. We then usually discard background stars which appear below the ZAMS and only retain stars which fulfil $M_G \leq 3 \times (G - J) + 2$ in the $M_G, G - J$ Colour-Magnitude-Diagram (CMD). Fourty stars are discarded by this criterium, all redder than $(G - J) = 1.0$. Since HSOY14 contains TGAS as a subset, we had to discard the above mentioned 35 TGAS stars from the remaining 109 stars. It turns out, however, that from the remaining 74 HSOY14 stars nine were also in the TGAS catalogue. Their proper motions differ slightly in the HSOY14 and TGAS catalogues, and this was a reason why they were not selected as TGAS candidates. Since the formal precision of the proper motions was a factor of almost two better for these stars in HSOY14 compared to TGAS, we kept them as kinematic candidates. Moreover, 7 out of 9 stars fulfilled the condition 2. These nine stars are given in the Table A.2.

As the remaining 65 faint HSOY14 candidates were only selected on the basis of their HSOY14 proper motions, we checked the data quality by cross-matching the stars with UCAC5 (Zacharias et al. 2017) for consistency. The reason for doing this is the following: the parent catalogue of HSOY is PPMXL which itself descends from USNO-B1.0 (Monet et al. 2003). South of -30° declination USNO-B1.0 is of poor quality, as the epoch difference between the first and the second epoch is low in the south, and a possible mismatching leads to grossly erroneous proper motions which may be handed over to HSOY. A comparison with a completely independent source such as UCAC5 removes this problem. So, we only retain those stars whose difference in proper motions between HSOY and UCAC5 is within $1\text{-}\sigma$ of the formal error of this difference. Thirty-two stars from 65 survived this check and are given in Table A.3 in the appendix.

3.1. Membership

Due to the selection procedure applied, our sample of kinematic candidates includes stars of different membership probability. The quality of membership is based mainly on the observations available for candidates that are consistent with the phase-space coordinates of the V1062 Sco MG defined by (1). If, as in the case of HSOY, only four parameters (α , δ , μ_α , μ_δ) are available and consistent with (1), we call these candidates m(4d) members. The CP method predicts parallax and radial velocity of candidate members. Both predictions have to be verified by observations. If no trigonometric parallaxes are available we can only make a negative selection by testing if the predicted absolute magnitudes are compatible with allowed stellar loci in CMDs. By doing this, we indeed classified a few m(4d) candidates as non-members due their location in CMDs (see Section 3.2)

However, the majority of our candidates had measurements of trigonometric parallaxes (ϖ_{trig}) or/and radial velocities (RV). If one of the quantities RV , or ϖ_{trig} is measured and consistent with (1), we called the star a m(5d) member since its five coordinates of the 6-D phase space coincide with the assumption of their membership in the moving group V1062 Sco. If RV and ϖ_{trig} were measured and fulfil (1), we call them m(6d) members. On the other hand, if one of the measurements was inconsistent with (1), we rejected this star as a member and call it non-member (nm).

In our total sample of 76 kinematic candidates of the V1062 Sco MG we found 12 m(6d) members. These are fully confirmed members and their existence proves the authenticity of the moving group. Also the 31 m(5d) members are very probable candidates, as their measured ϖ_{trig} confirms the predicted ϖ_{kin} from the CP method, or, in four cases, the measured RV confirm the predicted RV . The other 20 m(4d) candidates await confirmation by RV and ϖ_{trig} measurements. Finally, in three cases the predicted parallaxes were not confirmed by the observed ones, in one case RV was inconsistent, and one star was rejected due to both inconsistent parallax and radial velocity. At this point we want to emphasize that, using the photometric criteria, we also identified 8 m(4d) candidates as non-members (see the Section 3.2). An overview of the membership quality in the V1062 Sco moving group is given in Table 1.

The stars in our V1062 Sco MG are remarkably co-moving. Although we have allowed the component of the tangential velocity perpendicular to the direction to the convergent point to ± 3 km/s, we find an overall standard deviation as small as 1 km/s around the expectation value of zero. At 175 pc this corresponds to 0.83 mas/y, comparable to the accuracy of the TGAS proper motions. The corresponding scatter of the 12 m(6d) members

amounts to only 0.3 km/s or less than 0.3 mas/y comparable to the accuracy of the best TGAS stars. As the perpendicular component of the tangential velocity is a measure of the actual 1-d velocity dispersion in a cluster (moving group), we may safely conclude that it should be less than 1 km/s.

Table 1. Overview of the membership quality in the V1062 Sco moving group. In Column 1 we show the different membership qualities as explained in the Text, column 2 refers to TGAS stars from Table A.1, column 3 to HSOY stars with TGAS parallaxes (Table A.2), column 4 to HSOY stars (Table A.3). Finally, in column 5 we give the total number of stars with the respective membership quality.

Membership	Tab. A.1	Tab. A.2	Tab. A.3	all
m(6d)	11	1	-	12
m(5d) [$\varpi_{trig}/no RV$]	22	5	-	27
m(5d) [$RV/no \varpi_{trig}$]	-	-	4	4
m(4d)	-	-	20	20
nm	2	3	8	13
all	35	9	32	76

3.2. Colour-magnitude diagrams

All stars of the V1062 Sco MG as selected above have 2MASS (Skrutskie et al. 2006) photometry and Gaia DR1 (Gaia Collaboration et al. 2016) G -magnitudes. We present them in the colour-magnitude diagrams (CMDs) M_G vs. $G - J$ in Fig. 3 and M_{K_S} vs. $J - K_S$ in Fig. 4. The magnitudes on the ordinate are absolute magnitudes, and the colours on the abscissae are intrinsic colours in both diagrams. For the distance moduli we used the ϖ_{kin} , first because they are available for all the stars in the 3 tables, and second because, within the TGAS precision budget, they are formally more precise than the ϖ_{trig} . In any case the mean difference between the distance moduli from ϖ_{trig} and ϖ_{kin} is -0.01 mag with a standard deviation of 0.11 mag, so hardly visible on the plots. We also do not show error bars for the absolute magnitudes. For TGAS stars the median of the uncertainties in distance modulus is 0.1 mag based on kinematic, 0.17 mag on trigonometric parallaxes. For HSOY stars the median is 0.26 mag. All these quantities give error bars smaller than the size of the symbols. The reddening $E(B - V)$ was determined from photometric data on TGAS members since their actual distances are sufficiently well known from the trigonometric parallaxes. We obtained a value of 0.065 mag for $E(B - V)$ from the star's loci in the three CMDs, i.e., M_G vs. $G - J$, M_{K_S} vs. $J - K_S$ and M_V vs. $B - V$. Padova-2.8 Solar metallicity isochrones (Bressan et al. 2012) for $\log t = 6.6, 7.4$ and 8.0 are also shown in Figs. 3 and 4. From the distribution of the stars in both CMDs we estimate that the masses of our members range between $2.6 M_\odot$ to $0.7 M_\odot$.

It is conspicuous in both CMDs that the stars do not follow a unique isochrone, but are mainly located between isochrones of 4 Myrs and 25 Myr, especially those with spectral types later than about F0 ($J - K_S > 0.2$). This spread cannot be compensated by inaccuracy of photometric data: a typical rms -error is about 0.025 mag for J , K_S , and 0.01 mag for G -magnitudes. Also, binarity can alleviate the age discrepancy, but not completely remove it. A possible explanation can be that the stars have formed over a period of 20 Myrs, but are still moving together with the same space velocity. We remind the reader that the V1062 Sco MG is embedded in the Sco-Cen OB association, where many small star forming regions are present (see the discussion in the next section), but, to our knowledge, no one is found which is so nicely co-moving and well populated as the V1062 Sco MG.

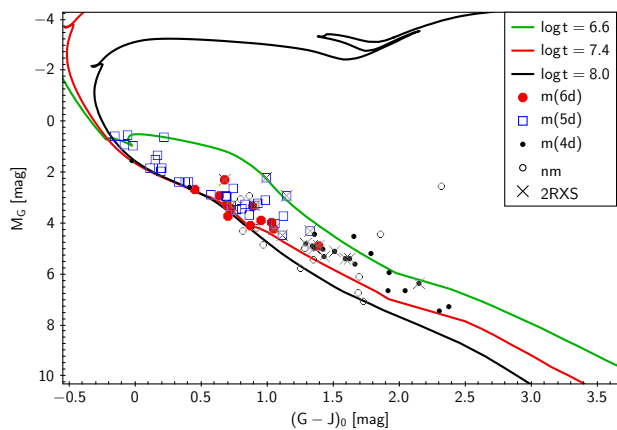


Fig. 3. The M_G vs. $(G - J)_0$ colour-magnitude diagram of stars in the V1062 Sco moving group. The symbols for the members of different membership quality are shown in the legend. Crosses mark stars that were observed by the ROSAT satellite (2RXS, see text). Also plotted are three Padova-2.8 Solar metallicity isochrones for $\log t = 6.6, 7.4$ and 8.0 .

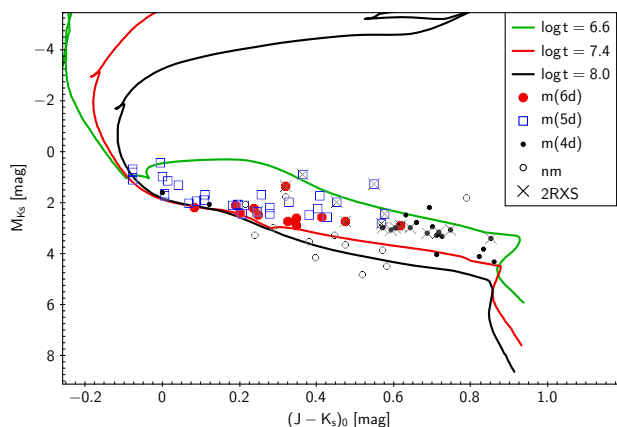


Fig. 4. The M_{K_S} vs. $(J - K_S)_0$ colour-magnitude diagram of stars in the V1062 Sco moving group. The symbols for the members of different membership quality are shown in the legend. Crosses mark stars that were observed by the ROSAT satellite (2RXS, see text). Also plotted are three Padova-2.8 Solar metallicity isochrones for $\log t = 6.6, 7.4$ and 8.0 .

We also tried to recover our stars in other sky surveys to get further indication on their youth. We found that eight TGAS stars (3 m(6d), 5 m(5d)) and nine HSOY14 stars (1 m(5d), 8 m(4d)) have ROSAT-2RXS (Boller et al. 2016) counterparts, but none of them is measured by Gaia (Morrissey et al. 2007) as our moving group is outside the area that Gaia observed.

As we mentioned above, the convergent point method predicts the parallaxes of the kinematic members. In contrast to TGAS candidates, we cannot yet verify the predictions for HSOY stars by measurements. Therefore, some few HSOY kinematic candidates may happen to be non-members of the V1062 Sco MG. We can decrease a possible contamination by checking the consistence of predicted parallaxes and photometric distances of m(4d) candidates. To be on a safe side, we marked a candidate as a non-member when it is located outside the area bordered by the isochrones $\log t = 6.6, 7.4$ in at least one of the CMDs (M_G vs. $G - J, M_{K_S}$ vs. $J - K_S$). Five of eight rejected candidates indeed seemed to be back- or foreground stars, whereas three others were probably main sequence stars at the distance of the V1062 Sco MG. In this case they may be co-moving field

stars older than 100 Myrs that are likely not connected to the young moving group V1062 Sco, i.e. "contaminants".

3.3. Estimate of the contamination

To estimate the number of field star contaminants that may enter our sample, we ran a Besançon simulation of the area around the cluster centre, obtaining a mock catalogue of field objects with 6D parameters. The Besançon simulation was performed over 40 square degrees with default parameters. The area was centered at $l = 343^\circ.7, b = +4^\circ.3$ and a constant extinction of $A_V = 1.2$ mag/kpc was added. This agrees with $A_V = 0.2$ mag at 175 pc, i.e. at the mean distance of the V1062 Sco MG where we estimated $E(B - V)$ to be 0.065 mag. We spread the mock positions over the whole area of 40 square degrees assuming a uniform distribution on the sky, the line-of-sight distance being determined by the Besançon simulator. The simulated cartesian parameters were converted into the observables, and we added Gaussian noise of 0.3 mas/yr (RMS) and 0.3 mas (RMS) on each proper motion component and the parallax, respectively. We also converted the Besançon Cousins photometry into the Gaia G system using the Jordi et al. (2010) colour transformation. Finally, to improve the statistics, we repeated the simulation ten times.

As for the real TGAS and HSOY14 stars, we ran the CP method around the phase-space coordinates (1) for this ten times enlarged simulation catalog. In Fig. 5 we show the simulated stars that came out from the CP method as kinematic candidates i.e., m(4d) members. In total, there are 64 stars in the area between the isochrones for $\log t = 6.6$ and $\log t = 7.4$. So, in fact, we expect a number of 7 (6.4) stars from the Besançon model to fall into the CMD area occupied by the stars from the V1062 Sco MG. In the following we give a worst case (maximum) estimate of the contamination: From our 68 kinematic candidates from Table 1 in the CMD area we had to discard already 5 as non-members based on discordant parallaxes or radial velocities. So, the maximum contamination among the remaining 63 is two, or 3%. In reality the contamination is much smaller for the m(5d) or m(6d) members. For instance, if we take into account the simulated parallaxes of the 6.4 contaminants, we find only 0.7 which should fall into the CMD area in Fig. 5.

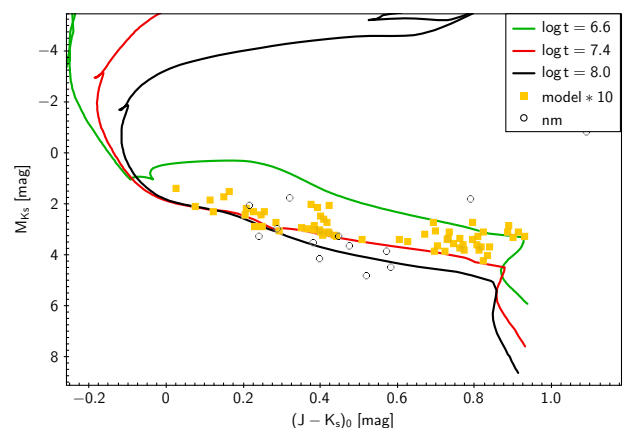


Fig. 5. The M_{K_S} vs. $(J - K_S)_0$ colour-magnitude diagram of stars in the area of the V1062 Sco MG obtained from a simulation based on the Besançon model (10-times enhanced). Again three Padova-2.8 Solar metallicity isochrones for $\log t = 6.6, 7.4$ and 8.0 are also given. Also plotted are the 13 non-members from Figures 3 and 4 and Table 1.

3.4. Individual stars

The star V1062 Sco (star 7 of our sample) is a variable of α_2 CVn type. Its TGAS parallax makes it an m(5d) member in our terminology. In the literature we found a radial velocity measurement of 13.00 ± 5.80 km/s from Levato et al. (1996). This radial velocity is almost $2\text{-}\sigma$ off the predicted radial velocity. However, in case of a rotationally variable stars it is hard to extract its line-of-sight velocity. Therefore we keep this star as an m(5d) member.

Star 5 (HD 149551) and star 18 (HD 150372) are found in Mamajek et al. (2002). Depending on different pMS isochrones the authors estimate an age between 4 and 11 Myrs and a mass between 1.5 and 1.7 M_{\odot} for star 5, and an age between 4 and 7 Myrs and a mass between 1.8 and 1.9 M_{\odot} for star 18. Star 9 (HD 149777) was rated 'active subgiant' by Mamajek et al. (2002) and hence rejected as a young member in the Sco-Cen association. However we keep it as a m(5d) member because of its measured trigonometric parallax. The preliminary velocity measurement ($RV = +0.6 \pm 7.8$ km/s) for this very rapidly rotation star ($v_{\text{rot}} \approx 200$ km/s) confirms its membership. Nevertheless the uncertainty of this measurement is rather large.

Star 30 of our sample (HD 152407) is mentioned in SIMBAD as a member in the cluster Trumpler 24. It has number 160 in the catalog of U, B, V measurements in Tr 24 by Heske & Wendker (1984). According to Heske & Wendker, TR 24 has a distance of 2300 pc, and they rate HD 152407 as a post-MS member from their photometry and give its spectral type of B5Ib. However, its trigonometric parallax of 5.48 mas clearly rules it out as a member in Tr 24, and sets doubts on its luminosity class Ib.

Star 141 of our sample is SZB86 from Song et al. (2012). They quote a distance of 99 pc, photometrically estimated from an empirical 10 Myr isochrone on an M_{K_s} versus $V - K_s$ CMD. They give a typical uncertainty of about 30% for their determination. This star is also found in Fuhrmeister & Schmitt (2003), in their catalog of X-ray variable stars as No. 844. They determine its spectral type to be M0Ve and rate it as a flare star. We keep this star as an m(4d) candidate, because of its kinematic distance of 175 pc.

Star 35 (HD 151738) is a spectroscopic binary with a difference in radial velocity of about 100 km/s. Because we do not know the mass ratio, we cannot use the measurement to constrain its membership.

Given the age range in V1062 Sco MG, we expect no detection of protoplanetary disks and very few detections of warm debris disks (Cieza et al. 2010). However, using VOSA (Bayo et al. 2008) we reveal a significant infrared excess in the WISE (Cutri & et al. 2012) bands for six targets: star 107 in W1 ($3.4\mu\text{m}$) redwards, stars 22, 124, and 143 in W3 ($12\mu\text{m}$) and W4 ($22\mu\text{m}$), and stars 26 and 59 in W4 only.

- Visual inspection of the relevant WISE images showed that stars 22 (HD 150532), 124 (2MASS 16375854-3933221) and 143 are associated with nebulosity both in W3 and W4 bands. Such complex backgrounds can lead to spurious detections (e.g. Cruz-Saenz de Miera et al. 2014). Actually we found no sources at the position of the stars in the W4 band images. The W3 band excess detections should also be taken carefully given the nebulosity.
- Star 107 (2MASS 16425498-4233057) was observed with the *Spitzer Space Telescope* using the IRAC instrument in the 3.6, 4.5, 5.8, and $8.0\mu\text{m}$ bands. These photometric data were taken from the Spitzer Enhanced Imaging Products cat-

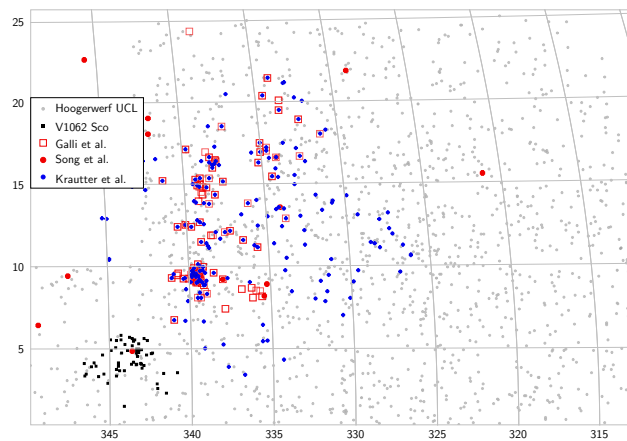


Fig. 6. The area of UCL in Galactic coordinates. The extent of UCL is outlined by the distribution of the stars from Hoogerwerf (2000), (grey dots). Our 63 members of the V1062 Sco MG are shown as black squares. Young stars from other authors in the UCL area are shown with the symbols indicated on the map.

alog (SEIP¹). In contrast to WISE observations, the analysis of IRAC data shows no evidence for excess between 3.6 and $8.0\mu\text{m}$. The reasons of these discrepancies are not yet clear.

- The IR excess of star 26 (HD 151109) was also detected by Rizzuto et al. (2012) and Chen et al. (2012). Based on photometric and spectroscopic observations with Spitzer, Chen et al. (2014) fitted the observed spectral shape of the excess using two blackbody components with temperatures of 237K and 91K. This two-component debris disk has a total fractional luminosity of 1.1×10^{-4} .
- The W4 band excess detection at star 59 (HD 152369) also seems to be solid.

None of those stars shows signs of accretion in our FEROS spectra. We ran a similar analysis on 221 random TGAS stars located at the same distance. None of those random stars showed consistent infrared excess as significant as our cluster members, giving a good hint that those disk detections may be real.

4. The V1062 Sco Moving Group and its relation to the Upper Centaurus Lupus association

The newly detected object is a co-moving group of young stars at the edge of the huge (845 deg^2) UCL association. The ages of the V1062 Sco MG members range from less than 10 to about 25 Myrs. Some of the younger stars were observed by the ROSAT satellite and show X-ray activity. The distance of the group from the Sun is 175 ± 7 pc. Within the UCL complex there are a number of areas where star formation has recently taken place or is still going on. These areas are related to dense molecular clouds in UCL and have been studied by a number of authors in the past decades. However, no evidence has been obtained for a compact moving group around the variable star V1062 Sco.

In his study of the Sco OB2_3 (UCL) area, Hoogerwerf (2000) searched for stars in the TRC catalog (Hog et al. 1998), a predecessor of Tycho-2, which had proper motions consistent with the spatial velocity of the Hipparcos members of UCL from de Zeeuw et al. (1999). Using a convergent-point method, with further constraints on the proper motion distribution, magnitude and colour, he found some 1200 candidate stars. Based

¹ http://irsa.ipac.caltech.edu/data/SPITZER/Enhanced/SEIP/docs/seip_explanato

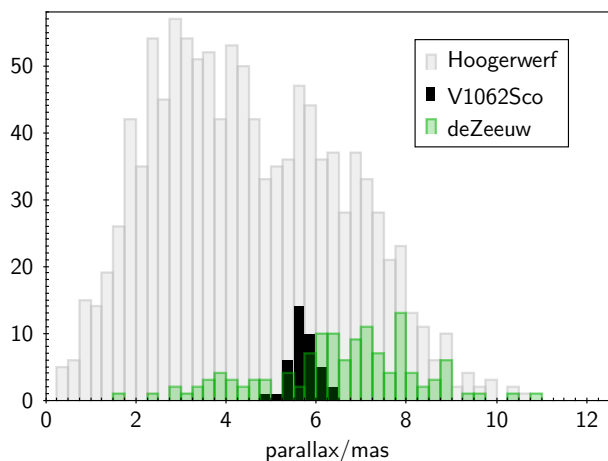


Fig. 7. Parallax distribution of stars in the UCL association. Grey bars show the TGAS parallaxes of the stars from Hoogerwerf (2000), green bars the Hipparcos stars from de Zeeuw et al. (1999). The black bars display the TGAS parallaxes of the 39 stars from Table 1 which are at least m(5d) members.

on Monte-Carlo simulations of the field star population he expected a contamination of between 400 and 800 field stars in this sample. He thus concluded that, among the 1200 stars, a considerable number of association members should be present which are fainter than the about 150 Hipparcos stars from de Zeeuw et al. (1999).

In Fig. 6, we show Hoogerwerf’s stars as small grey dots in the background. These stars outline the extent of the UCL area. From the 35 stars in Table A.1 27 are listed in Hoogerwerf (2000), but only six are also contained in de Zeeuw et al. (1999). Also six stars in Table A.2 and four in Table A.3 are included in Hoogerwerf (2000). We crossmatched the UCL association candidates with TGAS, and show in Fig. 7 their distribution versus the trigonometric parallaxes. They demonstrate a broad distribution with parallaxes between 1 mas and 10 mas. There is indicative of a bi-modal distribution with one part between 1 and 5 mas, probably the background field-star contaminants mentioned above, and between 5 and 8 mas of the UCL association proper. Also in Fig. 7 we show the distribution of the Hipparcos stars (but with TGAS parallaxes) from de Zeeuw et al. (1999). Their parallaxes are concentrated between 6 mas and 8 mas, showing a lower number of background contaminants. On top the parallax distributions in the UCL area in Fig. 7, we plot the distribution of TGAS parallaxes of our 39 stars from Table 1 which are at least m5d members. The V1062 Sco moving group members show a narrow parallax distribution clearly indicating a sub-condensation at the periphery of the UCL complex.

Based on X-ray data from the ROSAT All-Sky-Survey Krautter et al. (1997) discovered 136 new TTauri stars in the Lupus SFR (their tables 5, 6, and 11). The positions of these stars in UCL are also shown in Fig. 6. For 31 TTauri stars in Krautter et al. (1997) we identified TGAS counterparts. In comparison to our V1062 Sco MV members, they show a much wider parallax spread, between 5 and 11 mas with a peak at 7.5 mas (ca. 133 pc).

Song et al. (2012) have spectroscopically identified 100 G-, K-, and M-type members of the Scorpius-Centaurus complex. Sixteen of them are found in the UCL complex and are also plotted in Fig. 6. As already mentioned, their star SZB86 is an m(4d) kinematic member of our group (star 141). Song et al. (2012)

derived ages of about 10 Myr for stars in the Upper Centaurus Lupus region.

Galli et al. (2013) identified a comoving group with 109 pre-main sequence stars and candidates in the Lupus SFR. Assuming that all stars share the same space motion, they derived individual parallaxes for stars with known radial velocity and tentative parallaxes for the remaining group members. In their Fig. 3 they show the location of their UCL stars overplotted to the ^{12}CO intensity map from Tachihara et al. (2001). Galli et al. (2013) studied four sub-groups called Lupus 1 to Lupus 4, all associated with strong ^{12}CO emission. The average kinematic distances of these sub-groups range from 140 to 200 pc. Lupus 3, the most populated group at $(l, b) = (339^\circ 5', +9^\circ 5')$ in Fig. 6 has an average kinematic distance of 180 pc, but shows a considerable depth, i.e. the stars in Lupus 3 are located between 160 and 260 pc. Also the proper motions of this sample scatter between -5 and -35 mas/yr in both components. In a later paper, Galli et al. (2015) derived masses and ages of the TTS population in this SFR. The ages of their stars peak between 6 and 7 Myrs, and are, on average, younger than ours.

Unlike the other star forming regions in Lupus which are embedded in molecular clouds and show considerable scatter in their proper motions, the V1062 Sco MG is concentrated in a distance range between 165 and 185 pc, the scatter of its proper motions is comparable to the uncertainties of the proper motions in TGAS, resp. HSOY, and, finally, it is not embedded in a molecular cloud on the Tachihara et al. (2001) ^{12}CO map. In Section 3.2 we found a moderate value for $E(B - V)$, i.e. an A_V of about 0.2 mag in the direction of our group.

We additionally studied the interstellar-medium gas absorption in the NaI lines at 589.0 and 589.6 nm (Pascucci et al. 2015). Many of our targets show narrow-line absorption on top of the broad stellar absorption. These lines have a mean barycentric radial velocity of $+0.5$ km/s (in the LSR: $+6$ km/s), with an *rms*-spread of 2 km/s. Over most of the cluster, the stellar and gas RVs are very similar. While the RV spread is random on the sky, the depth of the absorption line is noticeably strong (mean of 71%) west of a great circle passing through $l, b = (343^\circ, +4^\circ)$, with an orientation of -10° (N to E), and small (mean of 31%) east of that line. This drop can be seen on the $\text{H}\alpha$ map of this velocity (HI4PI Collaboration et al. 2016). With these data, it is not possible to place the gas relative to the cluster and claim that the cluster still holds some of its original gas. We can however describe HI emission seen at other RV ($> +10$ km/s or < -2 km/s in the LSR) by the HI4PI Collaboration et al. (2016) as background gas.

5. Summary

The Upper Centaurus Lupus (UCL) subgroup of the Sco-Cen OB-association contains a large number of some 130 B and A stars at a mean distance of 140 pc from the Sun. Also it comprises a few subgroups, embedded in molecular clouds, where recent stars formation is going on. The new group around the variable star V1062 Sco is situated outside of these molecular clouds at a mean distance of 175 ± 7 pc from the Sun and contains 63 stars within a radius of 10 pc around the center. The stars in our moving group are not coeval, but show an age spread between 4 and 25 Myr for which we have no explanation. This group is strongly co-moving, the one-dimensional velocity dispersion being less than 1 km/s. The 33 members from the TGAS catalogue are selected such that the difference between their kinematic and trigonometric parallaxes is smaller than the $1-\sigma$ error of this difference. For a subset of 12 stars, we could confirm

a full 3-D coincidence of their space motion with the mean space motion of the group. These definitely form a moving group, or possibly an open cluster. For another subset of 27 stars the kinematically predicted parallaxes are confirmed by the trigonometric parallaxes from TGAS, they fulfil this necessary condition of being cluster members. Also four stars from HSOY have radial velocities confirmed. A last subset of 20 stars have predicted parallaxes consistent with the condition of co-movement. In total there are 63 stars belonging to this V1062 Sco moving group. A possible contamination by field stars is about 3% estimated on the basis of the Besançon model of our Galaxy. In summary, we have clearly shown that the V1062 Sco moving group is a new compact, young moving group within 200 pc from the Sun. The masses of our 63 members range from 2.6 M_{\odot} to 0.7 M_{\odot} . With Gaia data release 2, announced for April 2018 we expect to reveal new and fainter members of the group.

Acknowledgements. BG thanks Andres Jordan and Rafael Brahm for useful discussions and their help in reducing the FEROS data, as well as Caroline Bot and Jeroen Bouwman for their insights. The authors thank Ilaria Pascucci for her precious suggestions regarding IR excess and gas absorption. This study was supported by Sonderforschungsbereich SFB 881 "The Milky Way System" (subprojects B5 and B7) of the German Research Foundation (DFG). This research has made use of the SIMBAD database and of the Vizier catalogue access tool, operated at CDS, Strasbourg, France. This work has made use of data from the European Space Agency (ESA) mission *Gaia* (<https://www.cosmos.esa.int/gaia>), processed by the *Gaia* Data Processing and Analysis Consortium (DPAC, <https://www.cosmos.esa.int/web/gaia/dpac/consortium>). Funding for the DPAC has been provided by national institutions, in particular the institutions participating in the *Gaia* Multilateral Agreement. This publication makes use of VOSA, developed under the Spanish Virtual Observatory project supported from the Spanish MICINN through grant AyA2011-24052. This project has been supported by the Hungarian NKFI Grants K-115709 and K-119517 of the Hungarian National Research, Development and Innovation Office. AD was supported by the ÚNKP-17-4 New National Excellence Program of the Ministry of Human Capacities. AD would like to thank the City of Szombathely for support under Agreement No. 67.177-21/2016. We would like to thank the anonymous referee for her/his very constructive and helpful comments.

References

- Altmann, M., Roeser, S., Demleitner, M., Bastian, U., & Schilbach, E. 2017, *A&A*, 600, L4
- Bayo, A., Rodrigo, C., Barrado Y Navascués, D., et al. 2008, *A&A*, 492, 277
- Blaauw, A. 1964, *ARA&A*, 2, 213
- Boller, T., Freyberg, M. J., Trümper, J., et al. 2016, *A&A*, 588, A103
- Brahm, R., Hartman, J. D., Jordan, A., et al. 2017, *ArXiv e-prints* [[arXiv:1707.07093](https://arxiv.org/abs/1707.07093)]
- Brahm, R., Jordan, A., Hartman, J., & Bakos, G. 2016, ZASPE: Zonal Atmospheric Stellar Parameters Estimator, Astrophysics Source Code Library
- Bressan, A., Marigo, P., Girardi, L., et al. 2012, *MNRAS*, 427, 127
- Chen, C. H., Mittal, T., Kuchner, M., et al. 2014, *ApJS*, 211, 25
- Chen, C. H., Pecaut, M., Mamajek, E. E., Su, K. Y. L., & Bitner, M. 2012, *ApJ*, 756, 133
- Cieza, L. A., Schreiber, M. R., Romero, G. A., et al. 2010, *ApJ*, 712, 925
- Cruz-Saenz de Miera, F., Chavez, M., Bertone, E., & Vega, O. 2014, *MNRAS*, 437, 391
- Cutri, R. M. & et al. 2012, *VizieR Online Data Catalog*, 2311
- de Zeeuw, P. T., Hoogerwerf, R., de Bruijne, J. H. J., Brown, A. G. A., & Blaauw, A. 1999, *AJ*, 117, 354
- Fuhrmeister, B. & Schmitt, J. H. M. M. 2003, *A&A*, 403, 247
- Gaia Collaboration, Brown, A. G. A., Vallenari, A., et al. 2016, *A&A*, 595, A2
- Gaia Collaboration, van Leeuwen, F., Vallenari, A., et al. 2017, *A&A*, 601, A19
- Galli, P. A. B., Bertout, C., Teixeira, R., & Ducourant, C. 2013, *A&A*, 558, A77
- Galli, P. A. B., Bertout, C., Teixeira, R., & Ducourant, C. 2015, *A&A*, 580, A26
- Gilmore, G., Randich, S., Asplund, M., et al. 2012, *The Messenger*, 147, 25
- Goldman, B., Röser, S., Schilbach, E., et al. 2013, *A&A*, 559, A43
- Heske, A. & Wendker, H. J. 1984, *A&AS*, 57, 205
- HI4PI Collaboration, Ben Bekhti, N., Flöer, L., et al. 2016, *A&A*, 594, A116
- Hog, E., Kuzmin, A., Bastian, U., et al. 1998, *A&A*, 335, L65
- Hoogerwerf, R. 2000, *MNRAS*, 313, 43
- Jordi, C., Gebran, M., Carrasco, J. M., et al. 2010, *A&A*, 523, A48
- Kaufer, A., Stahl, O., Tubbesing, S., et al. 1999, *The Messenger*, 95, 8
- Krautter, J., Wichmann, R., Schmitt, J. H. M. M., et al. 1997, *A&AS*, 123
- Larson, R. B. 2002, in *Astronomical Society of the Pacific Conference Series*, Vol. 285, *Modes of Star Formation and the Origin of Field Populations*, ed. E. K. Grebel & W. Brandner, 442
- Levato, H., Malaroda, S., Morrell, N., Solivella, G., & Grosso, M. 1996, *A&AS*, 118, 231
- Lindegren, L., Lammers, U., Bastian, U., et al. 2016, *A&A*, 595, A4
- Mamajek, E. E., Meyer, M. R., & Liebert, J. 2002, *AJ*, 124, 1670
- Mayor, M., Pepe, F., Queloz, D., et al. 2003, *The Messenger*, 114, 20
- Michalik, D., Lindegren, L., & Hobbs, D. 2015, *A&A*, 574, A115
- Monet, D. G., Levine, S. E., Canzian, B., et al. 2003, *AJ*, 125, 984
- Morrissey, P., Conrow, T., Barlow, T. A., et al. 2007, *ApJS*, 173, 682
- Oh, S., Price-Whelan, A. M., Hogg, D. W., Morton, T. D., & Spergel, D. N. 2017, *AJ*, 153, 257
- Pascucci, I., Edwards, S., Heyer, M., et al. 2015, *ApJ*, 814, 14
- Randich, S., Tognelli, E., Jackson, R., et al. 2017, *ArXiv e-prints* [[arXiv:1711.07699](https://arxiv.org/abs/1711.07699)]
- Rizzuto, A. C., Ireland, M. J., & Zucker, D. B. 2012, *MNRAS*, 421, L97
- Röser, S., Schilbach, E., & Goldman, B. 2016, *A&A*, 595, A22
- Röser, S., Schilbach, E., Piskunov, A. E., Kharchenko, N. V., & Scholz, R.-D. 2011, *A&A*, 531, A92+
- Santos, N. C., Sousa, S. G., Mortier, A., et al. 2013, *A&A*, 556, A150
- Skrutskie, M. F., Cutri, R. M., Stiening, R., et al. 2006, *AJ*, 131, 1163
- Song, I., Zuckerman, B., & Bessell, M. S. 2012, *AJ*, 144, 8
- Tachihara, K., Toyoda, S., Onishi, T., et al. 2001, *PASJ*, 53, 1081
- Zacharias, N., Finch, C., & Frouard, J. 2017, *AJ*, 153, 166

Appendix A: Tables

Table A.1. TGAS stars in the V1062 Sco moving group.

The columns of the table give: Col. 1 the internal star number in the V1062Sco MG, col. 2 the main identifier of the star in SIMBAD. Cols. 3 and 4 the right ascension and declination, cols. 5 and 6 the proper motions in right ascension and declination in the TGAS catalog. Col. 7 the kinematic parallax and its mean error from the CP method, col. 8 the trigonometric parallax and its mean error from TGAS. Cols. 9 to 11 the J, H, K_s magnitudes from 2MASS, col. 12 the mean G -magnitude from Gaia DR1, col. 13 gives the membership information (and comments), cols. 14 to 16 the cross-match with de Zeeuw et al. (1999), Hoogerwerf (2000) and ROSAT-2RXS (Boller et al. 2016).

nr	Name	RA (J2000) (deg)	DEC (J2000) (deg)	μ_α (mas/y)	μ_δ (mas/y)	$\varpi_{\text{kin.}}$ (mas)	ϖ_{TGAS} (mas)	J (mag)	H (mag)	K_s (mag)	G (mag)	Membership	Z	H	X
1	HD 149354	248.980605	-40.333009	-14.11	-20.41	5.69±0.29	5.53±0.44	8.542	8.266	8.178	9.589	m(5d)	-	H	-
2	HD 149425	249.119405	-40.303120	-11.92	-20.84	5.52±0.01	5.71±0.51	6.744	6.781	6.714	7.075	m(5d)	Z	H	-
3	HD 149467	249.182939	-39.332763	-12.79	-20.90	5.62±0.32	5.50±0.25	8.738	8.517	8.426	9.685	m(5d)	-	H	-
4	HD 149533	249.260954	-38.676307	-12.53	-20.98	5.61±0.01	6.30±0.42	7.268	7.273	7.233	7.372	m(5d)	-	H	-
5	HD 149551	249.303557	-39.010658	-11.62	-21.03	5.51±0.02	5.76±0.39	8.453	8.103	8.010	9.553	m(5d)	Z	H	-
6	TYC 7858-585-1	249.425372	-40.171494	-11.55	-21.04	5.51±0.50	6.01±0.92	9.273	8.943	8.826	10.426	m(6d)	-	-	-
7	V* V1062 Sco	249.628854	-39.152419	-12.58	-21.21	5.66±0.01	5.82±0.44	6.883	6.927	6.926	6.941	m(5d)	-	H	-
8	HD 149726	249.630042	-41.635380	-13.67	-21.19	5.80±0.03	6.24±0.28	8.488	8.325	8.270	9.302	m(5d)	-	H	-
9	HD 149777	249.660225	-39.551078	-11.83	-21.02	5.54±0.02	5.69±0.39	7.561	7.280	7.161	8.670	m(5d)	-	H	X
10	HD 149793	249.681434	-39.679564	-13.07	-22.60	6.00±0.35	5.55±0.22	8.618	8.420	8.345	9.625	m(6d)	-	H	-
11	HD 149938	249.888793	-39.609281	-12.16	-21.14	5.60±0.12	5.49±0.36	7.939	7.891	7.898	8.260	m(5d)	-	H	-
12	HD 150004	249.991238	-39.789033	-12.11	-20.68	5.50±0.09	5.54±0.34	7.499	7.494	7.451	7.785	m(5d)	-	H	-
13	HD 150107	250.137078	-38.226872	-11.95	-22.55	5.85±0.27	5.63±0.31	8.785	8.603	8.548	9.598	m(6d)	-	H	-
14	HD 150092	250.217787	-40.433294	-13.04	-22.30	5.94±0.60	6.19±0.89	9.099	8.824	8.716	10.169	m(6d)	-	H	-
15	HD 150196	250.284884	-40.225852	-12.56	-21.31	5.68±0.29	5.59±0.26	8.970	8.737	8.686	9.809	m(6d)	-	H	-
16	HD 150287	250.466614	-40.466324	-11.76	-21.41	5.61±0.02	5.79±0.28	8.581	8.388	8.357	9.338	m(6d)	Z	H	-
17	TYC 7871-694-1	250.500567	-40.049478	-11.71	-21.39	5.60±0.63	5.67±0.29	9.812	9.312	9.159	11.318	m(6d)	-	-	X
18	HD 150372	250.599928	-40.058326	-10.59	-22.63	5.72±0.27	5.30±0.48	8.047	7.614	7.464	9.310	m(5d)	-	-	X
19	HD 321892	250.613520	-38.460159	-12.91	-21.52	5.75±0.42	5.84±0.23	8.642	8.245	8.156	9.660	m(5d)	-	H	X
20	HD 150398	250.627049	-38.930180	-11.28	-21.87	5.64±0.23	5.80±0.25	8.522	8.433	8.404	9.092	m(6d)	-	H	-
21	HD 325907	250.631351	-41.759400	-12.43	-22.55	5.93±0.45	5.53±0.25	9.416	9.090	9.034	10.401	m(6d)	-	-	-
22	HD 150532	250.872192	-41.986154	-9.54	-24.10	5.92±0.31	5.70±0.24	8.802	8.679	8.561	9.725	m(5d)	-	H	-
23	HD 150989	251.554962	-39.745820	-11.99	-22.91	5.93±0.17	5.91±0.30	8.182	8.128	8.040	8.680	m(5d)	-	H	-
24	HD 150988	251.570570	-39.272726	-11.43	-22.03	5.69±0.10	5.67±0.35	7.987	7.971	7.946	8.215	m(5d)	-	H	-
25	HD 321958	251.667832	-38.147518	-11.83	-21.74	5.67±0.62	5.91±0.25	9.452	9.030	8.942	10.621	m(6d)	-	-	X
26	HD 151109	251.756929	-39.533964	-11.59	-21.97	5.70±0.01	4.96±0.91	6.998	7.038	7.039	6.963	m(5d)	Z	H	-
27	HD 151681	252.602617	-38.048545	-12.45	-22.22	5.83±0.13	5.82±0.30	7.982	7.968	7.838	8.295	m(5d)	-	H	-
28	HD 151726	252.689598	-38.256513	-11.79	-22.70	5.86±0.01	5.69±0.39	7.218	7.261	7.261	7.257	m(5d)	Z	-	-
29	HD 152041	253.173750	-38.760443	-11.32	-22.02	5.67±0.02	5.38±0.37	7.913	7.727	7.558	8.706	m(6d)	Z	H	X
30	HD 152407	253.743519	-41.092913	-12.90	-21.79	5.80±0.20	5.48±0.37	8.213	8.155	8.089	8.735	m(5d)	-	H	-
31	HD 321803	248.548464	-39.626711	-9.30	-22.78	5.60±1.28	6.32±0.23	9.271	8.965	8.809	10.442	m(5d)	-	H	-
32	HD 149230	248.827830	-42.239950	-12.99	-21.23	5.74±0.27	5.42±0.39	8.495	8.383	8.265	9.294	m(5d)	-	H	-
33	TYC 7358-330-1	249.948782	-36.609805	-11.92	-22.38	5.80±0.80	2.15±0.27	9.909	9.594	9.427	11.311	nm (kin)	-	-	-
34	HD 325890	250.201816	-41.271889	-9.78	-24.05	5.92±0.35	3.13±0.26	9.450	9.222	9.129	10.487	nm (kin), binary	-	-	-
35	HD 151738	252.742709	-38.928093	-11.13	-21.13	5.47±0.32	5.48±0.27	8.935	8.717	8.656	9.781	m(5d), binary	-	H	X

Table A.2. TGAS stars with HSOY proper motions in the V1062 Sco moving group.

The columns of the table give: Col. 1 the internal star number in the V1062Sco MG, col. 2 the main identifier of the star in SIMBAD. Cols. 3 and 4 the right ascension and declination, cols. 5 and 6 the proper motions in right ascension and declination in the HSOY catalog. Col. 7 the kinematic parallax and its mean error from the CP method, col. 8 the trigonometric parallax and its mean error from TGAS. Cols. 9 to 11 the J, H, K_s magnitudes from 2MASS, col. 12 the mean G -magnitude from Gaia DR1, col. 13 gives the membership information (and comments), cols. 14 and 15 the cross-match with Hoogerwerf (2000) and ROSAT-2RXS (Boller et al. 2016).

nr	Name	RA (J2000) (deg)	DEC (J2000) (deg)	μ_α (mas/y)	μ_δ (mas/y)	$\varpi^{\text{kin.}}$ (mas)	ϖ^{TGAS} (mas)	J (mag)	H (mag)	K_s (mag)	G (mag)	Membership	H	X
51	HD 149638	249.429970	-39.708627	-13.21	-20.97	5.69 ± 0.23	5.71 ± 0.22	8.862	8.539	8.425	10.097	m(5d)	H	-
52	HD 150165	250.234747	-40.187218	-11.27	-22.49	5.77 ± 0.15	5.83 ± 0.28	8.304	8.049	7.950	9.280	nm (kin)	H	-
53	HD 149738	249.612316	-39.651811	-11.73	-20.80	5.48 ± 0.06	6.07 ± 0.32	7.683	7.658	7.607	7.955	m(5d)	H	-
54	HD 322024	251.071987	-40.252976	-14.11	-20.20	5.63 ± 0.25	0.71 ± 0.87	6.533	5.687	5.410	8.967	nm (kin)	-	-
55	HD 149336	248.895070	-37.110095	-11.44	-22.61	5.80 ± 0.15	6.17 ± 0.25	8.486	8.249	8.237	9.399	nm (RV)	H	-
56	HD 149984	249.946029	-38.769026	-13.02	-21.86	5.83 ± 0.22	5.79 ± 0.22	9.232	8.951	8.872	10.051	m(6d)	H	-
57	HD 321981	251.376202	-39.161844	-11.63	-21.44	5.59 ± 0.24	5.00 ± 0.38	9.300	8.787	8.690	10.741	m(5d)	-	X
58	HD 151868	252.940040	-38.052476	-12.32	-21.31	5.63 ± 0.18	5.90 ± 0.22	8.593	8.427	8.345	9.281	m(5d)	-	-
59	HD 152369	253.642044	-38.105640	-12.05	-22.56	5.85 ± 0.09	6.24 ± 0.92	8.262	8.204	8.159	8.710	m(5d)	H	-

Table A.3. HSOY stars in the V1062 Sco moving group.

The columns of the table give: Col. 1 the internal star number in the V1062Sco MG, col. 2 the main identifier of the star in SIMBAD, resp. the 2MASS identifier. Cols. 3 and 4 the right ascension and declination, cols. 5 and 6 the proper motions right ascension and declination in the HSOY catalog. Col. 7 the kinematic parallax and its mean error from the CP method. Cols. 8 to 10 the J, H, K_s magnitudes from 2MASS, col. 11 the mean G -magnitude from Gaia DR1, cols. 12 and 13 give the membership information and comments, cols. 14 and 15 the cross-match with Hoogerwerf (2000) and ROSAT-2RXS (Boller et al. 2016).

nr	Name	RA (J2000) (deg)	DEC (J2000) (deg)	μ_α (mas/y)	μ_δ (mas/y)	$\varpi_{\text{kin.}}$ (mas)	J (mag)	H (mag)	K_s (mag)	G (mag)	Membership	H	X
101	16365957-4137069	249.248204	-41.618651	-12.05	-21.72	5.72±0.68	11.292	10.796	10.676	13.093	nm	-	-
103	16302731-3915237	247.613815	-39.256619	-11.91	-21.48	5.64±0.68	11.624	11.235	11.070	13.463	nm	-	-
105	16342105-3922198	248.587707	-39.372174	-12.15	-22.25	5.82±0.81	10.049	9.448	9.297	11.754	m(4d)	-	X
107	16425498-4233057	250.729102	-42.551605	-10.65	-22.76	5.78±0.69	11.159	10.556	10.303	13.646	m(4d)	-	-
112	16442615-4218387	251.108983	-42.310795	-11.00	-21.57	5.57±0.26	10.849	10.503	10.418	12.212	nm	-	-
116	HD 321880	249.950060	-40.311165	-13.85	-22.12	5.99±0.25	8.733	8.089	7.911	10.704	nm (phot,RV)	-	-
119	16410838-4016078	250.284907	-40.268874	-12.03	-20.87	5.53±0.27	9.924	9.431	9.248	11.547	m(4d)	-	X
122	16383616-3937478	249.650689	-39.629952	-12.38	-20.76	5.55±0.25	9.932	9.331	9.198	11.467	m(4d)	-	-
123	16380672-3935178	249.528017	-39.588301	-13.72	-21.53	5.86±0.29	10.152	9.619	9.407	11.933	m(4d)	-	-
124	16375854-3933221	249.493986	-39.556155	-14.82	-21.77	6.03±0.35	10.769	10.069	9.902	12.929	m(4d)	-	-
125	TYC 7858-310-1	249.571281	-39.470607	-12.16	-21.26	5.62±0.21	9.125	8.790	8.711	10.105	m(5d) w/RV	-	-
126	HD 321933	250.560323	-39.863465	-13.41	-21.38	5.79±0.24	9.577	9.105	8.974	10.809	m(5d) w/RV	-	X
127	TYC 7871-176-1	250.776195	-39.812497	-13.02	-21.30	5.72±0.25	9.880	9.355	9.254	11.351	m(4d)	-	X
134	16532843-4057025	253.368481	-40.950717	-9.81	-22.20	5.56±0.25	9.796	9.597	9.520	10.730	nm	-	-
137	16325443-3843525	248.226801	-38.731281	-11.21	-21.98	5.65±0.69	10.679	10.240	10.073	12.490	nm	-	-
138	16363904-3902277	249.162655	-39.041054	-13.57	-20.87	5.71±0.27	9.680	9.116	8.987	11.582	m(4d)	-	-
139	HD 149491	249.215949	-38.862775	-12.61	-21.59	5.74±0.21	8.946	8.761	8.634	9.827	m(5d) w/RV	H	-
140	HD 321858	249.813745	-39.385783	-12.30	-21.90	5.77±0.25	9.333	8.852	8.668	10.805	m(4d)	-	-
141	[SZB2012] 86	249.947147	-39.344561	-11.46	-22.04	5.70±0.81	10.490	9.753	9.604	12.754	m(4d)	-	X
142	TYC 7867-1825-1	250.205341	-39.174494	-9.27	-23.79	5.80±0.27	10.313	9.942	9.803	11.780	nm	-	-
143	16403359-3907217	250.140032	-39.122720	-13.63	-20.97	5.73±0.69	11.402	10.736	10.507	13.814	m(4d)	-	-
144	16392813-3824231	249.867256	-38.406428	-11.83	-21.33	5.59±0.26	9.824	9.352	9.220	11.233	m(4d)	-	X
148	16485929-3935423	252.247050	-39.595075	-9.65	-22.39	5.57±0.29	10.092	9.509	9.311	11.827	m(4d)	-	X
149	16472452-3918481	251.852162	-39.313364	-10.33	-21.67	5.50±0.26	9.919	9.439	9.281	11.375	m(4d)	-	X
151	16382553-3813591	249.606386	-38.233091	-12.90	-22.16	5.88±0.27	10.219	9.656	9.461	12.256	m(4d)	-	-
152	HD 150641	250.985442	-38.333792	-13.10	-21.76	5.82±0.08	7.804	7.826	7.768	7.898	m(4d)	H	-
154	16413760-3753488	250.406681	-37.896899	-13.62	-21.25	5.77±0.26	10.100	9.520	9.380	11.648	m(4d)	-	X
158	TYC 7868-100-1	252.507688	-37.839328	-10.43	-23.17	5.80±0.25	10.097	9.777	9.681	11.179	nm	-	-
159	16522966-3928195	253.123626	-39.472107	-12.02	-20.84	5.51±0.72	11.069	10.460	10.323	13.098	m(4d)	-	-
161	TYC 7868-489-1	253.812634	-38.099953	-11.95	-21.80	5.69±0.24	9.136	8.522	8.411	10.906	m(4d)	-	X
164	HD 152001	253.103891	-37.607453	-11.90	-22.40	5.80±0.08	8.395	8.250	8.238	8.926	m(4d)	H	-
165	HD 150439	250.685374	-38.955712	-15.06	-21.99	6.09±0.14	8.036	7.829	7.745	8.891	m(5d) w/RV	H	n

Table A.4. FEROS observation log. For each spectrum, we list the modified barycentric Julian Day, the integration time, the SNR at 515 nm, the radial velocity, the bisector value if it could be measured, and the width of the CCF peak.

nr	MBJD	exp.time (s)	SNR (at 515 nm)	RV (km/s)	Bisector	CCFwidth (Å)
6	57 952.080 29	300	71	+3.61±0.21	-1.755±0.011	29.5
10	57 952.137 38	300	130	+2.40±0.10	—	23.4
13	57 952.174 75	300	127	+1.53±0.07	—	19.1
14	57 952.181 16	300	89	+1.79±0.02	0.052±0.010	8.1
15	57 952.197 83	300	108	+1.95±0.10	—	20.6
16	57 952.204 20	300	138	+3.64±0.31	1.542±0.008	28.8
17	57 952.219 87	300	39	+2.41±0.04	—	11.2
17	57 952.228 80	600	50	+2.42±0.03	-0.032±0.015	11.2
20	57 953.111 31	300	159	+2.49±0.10	—	24.8
21	57 953.130 64	300	79	+2.97±0.06	—	14.8
25	57 953.174 48	600	91	+1.03±0.02	-0.115±0.010	10.6
25	57 953.168 68	300	62	+1.11±0.03	-0.113±0.013	10.7
29	57 953.214 03	300	165	+2.07±0.36	-0.118±0.007	29.1
34	57 954.143 86	300	82	-79.66±0.04	0.047±0.011	6.1
34	57 954.135 72	300	79	-79.19±0.04	0.158±0.011	6.1
34	57 954.147 92	300	79	-79.79±0.04	0.142±0.011	6.1
34	57 954.139 80	300	82	-79.35±0.04	0.106±0.011	6.1
35	57 954.256 78	300	73	+7.02±6.91	—	46.6
35	57 954.260 84	300	74	-0.77±6.78	0.122±0.011	46.9
35	57 954.252 72	300	96	+7.60±5.56	0.352±0.010	47.5
55	57 954.047 46	300	152	-33.30±0.02	0.939±0.008	10.4
55	57 954.043 41	300	149	-33.23±0.02	—	10.5
55	57 954.039 35	300	143	-33.24±0.02	—	10.5
56	57 954.091 13	300	102	+1.74±0.05	—	14.3
56	57 954.095 21	300	105	+1.83±0.05	—	14.3
56	57 954.099 25	300	97	+1.73±0.05	-0.202±0.010	14.3
116	57 954.120 32	300	52	-66.09±0.01	0.003±0.014	4.5
116	57 954.112 17	300	53	-65.97±0.01	-0.148±0.014	4.6
116	57 954.116 25	300	53	-66.06±0.01	0.054±0.014	4.5
116	57 954.108 11	300	53	-66.08±0.01	0.093±0.014	4.5
120	57 954.227 16	300	171	-46.60±0.01	0.055±0.007	5.2
120	57 954.222 92	300	176	-46.60±0.01	0.042±0.007	5.2
125	57 954.085 64	300	102	-3.18±0.01	0.025±0.009	4.4
125	57 954.081 59	300	102	-3.15±0.01	0.070±0.009	4.4
125	57 954.077 54	300	102	-3.14±0.01	0.077±0.009	4.4
126	57 954.187 53	300	32	+6.43±0.02	0.102±0.020	5.9
126	57 954.175 33	300	64	+6.21±0.01	0.135±0.012	6.0
126	57 954.179 40	300	62	+6.29±0.01	0.129±0.013	6.1
126	57 954.183 47	300	56	+6.22±0.01	0.069±0.013	6.1
139	57 954.061 48	300	124	+5.13±0.06	0.126±0.009	16.6
139	57 954.057 41	300	127	+5.10±0.06	—	16.5
139	57 954.053 36	300	127	+5.06±0.06	—	16.5
165	57 954.208 70	300	89	+1.62±0.11	—	20.7
165	57 954.217 00	300	118	+1.46±0.08	—	20.8
165	57 954.212 93	300	97	+1.51±0.10	—	20.7
165	57 954.204 64	300	79	+1.14±0.11	—	20.6

Table A.5. Astrophysical parameters of member stars in the V1062 Sco moving group, followed by 4 rejected candidates. The measurements are weighted averages when multiple spectra were observed. In this case the uncertainties are the error on the mean. RV from the CERES pipeline, stellar parameters from ZASPE.

nr	RV (km/s)	T_{eff} (K)	$\log g$	$v \sin i$ (km/s)	[Fe/H]
6	+3.61±0.21	6026	3.8	51.8	+0.22
10	+2.40±0.10	6295	3.8	38.8	-0.02
13	+1.53±0.07	6406	3.9	31.5	+0.08
14	+1.79±0.02	5772	4.1	12.3	+0.04
15	+1.95±0.10	6387	3.8	33.8	+0.04
16	+3.64±0.31	6702	3.8	66.8	+0.10
17	+2.41±0.02	5032	4.0	17.0	+0.16
20	+2.49±0.10	5882	2.5	37.1	-0.52
21	+2.97±0.06	—	—	—	—
25	+1.06±0.02	5332	4.2	16.7	+0.05
29	+2.07±0.36	6197	4.0	79.2	-0.04
56	+1.77±0.03	6144	4.0	23.5	+0.04
125	-3.16±0.01	6254	4.3	4.9	+0.03
126	+6.26±0.01	5336	4.2	8.1	+0.03
139	+5.10±0.03	6383	3.9	27.5	+0.01
165	+1.45±0.05	6204	3.9	33.2	+0.08
35	—	6020	3.5	119.9	+0.15
34	-79.50±0.02	6790	3.6	8.8	-0.52
55	-33.26±0.01	6508	4.3	17.0	+0.17
116	-66.05±0.01	5022	2.7	5.0	-0.37
120	-46.60±0.00	—	—	—	—